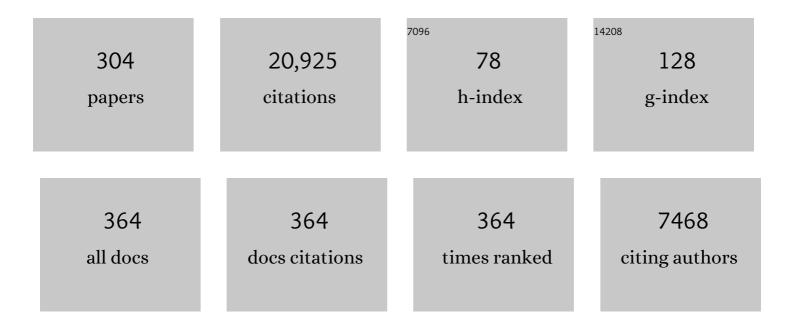
Taras Gerya

List of Publications by Year in descending order

Source: https://exaly.com/author-pdf/2903716/publications.pdf Version: 2024-02-01



TADAS CEDVA

#	Article	IF	CITATIONS
1	The rise and demise of deep accretionary wedges: A long-term field and numerical modeling perspective. , 2022, 18, 69-103.		9
2	Numerical modeling of subduction: State of the art and future directions. , 2022, 18, 503-561.		22
3	Self-organization of magma supply controls crustal thickness variation and tectonic pattern along melt-poor mid-ocean ridges. Earth and Planetary Science Letters, 2022, 584, 117482.	4.4	5
4	Subduction earthquake sequences in a non-linear visco-elasto-plastic megathrust. Geophysical Journal International, 2022, 229, 1098-1121.	2.4	10
5	Contrasting influence of sediments vs surface processes on retreating subduction zones dynamics. Tectonophysics, 2022, 836, 229410.	2.2	3
6	Low-degree mantle melting controls the deep seismicity and explosive volcanism of the Gakkel Ridge. Nature Communications, 2022, 13, .	12.8	8
7	A Wavelet-Based Adaptive Finite Element Method for the Stokes Problems. Fluids, 2022, 7, 221.	1.7	Ο
8	Subduction earthquake cycles controlled by episodic fluid pressure cycling. Lithos, 2022, 426-427, 106800.	1.4	12
9	Physics-Based Numerical Modeling of Geological Processes. , 2021, , 868-883.		1
10	Subduction Initiation. , 2021, , 994-1000.		1
11	Plumeâ€Induced Sinking of Intracontinental Lithospheric Mantle: An Overlooked Mechanism of Subduction Initiation?. Geochemistry, Geophysics, Geosystems, 2021, 22, e2020GC009482.	2.5	27
12	Transition from continental rifting to oceanic spreadingÂin the northern Red SeaÂarea. Scientific Reports, 2021, 11, 5594.	3.3	11
13	Trans-lithospheric diapirism explains the presence of ultra-high pressure rocks in the European Variscides. Communications Earth & Environment, 2021, 2, .	6.8	24
14	Time will tell: Secular change in metamorphic timescales and the tectonic implications. Gondwana Research, 2021, 93, 291-310.	6.0	24
15	Backarc Lithospheric Thickness and Serpentine Stability Control Slabâ€Mantle Coupling Depths in Subduction Zones. Geochemistry, Geophysics, Geosystems, 2021, 22, e2020GC009304.	2.5	10
16	Controls by rheological structure of the lithosphere on the temporal evolution of continental magmatism: Inferences from the Pannonian Basin system. Earth and Planetary Science Letters, 2021, 565, 116925.	4.4	20
17	Transient Slow Slip Characteristics of Frictionalâ€Viscous Subduction Megathrust Shear Zones. AGU Advances, 2021, 2, e2021AV000416.	5.4	11
18	Oblique subduction and mantle flow control on upper plate deformation: 3D geodynamic modeling. Earth and Planetary Science Letters, 2021, 569, 117056.	4.4	16

#	Article	IF	CITATIONS
19	Plate motion and plume-induced subduction initiation. Gondwana Research, 2021, 98, 277-288.	6.0	5
20	Depletion of the upper mantle by convergent tectonics in the Early Earth. Scientific Reports, 2021, 11, 21489.	3.3	5
21	Plume-Induced Subduction Initiation: Revisiting Models and Observations. Frontiers in Earth Science, 2021, 9, .	1.8	13
22	Dynamic slab segmentation due to brittle–ductile damage in the outer rise. Nature, 2021, 599, 245-250.	27.8	41
23	Inversion in the permeability evolution of deforming Westerly granite near the brittle–ductile transition. Scientific Reports, 2021, 11, 24027.	3.3	0
24	Building cratonic keels in Precambrian plate tectonics. Nature, 2020, 586, 395-401.	27.8	43
25	Corona structures driven by plume–lithosphere interactions and evidence for ongoing plume activity on Venus. Nature Geoscience, 2020, 13, 547-554.	12.9	90
26	Seismo-hydro-mechanical modelling of the seismic cycle: Methodology and implications for subduction zone seismicity. Tectonophysics, 2020, 791, 228504.	2.2	25
27	Slab Rollback Orogeny Model: A Test of Concept. Geophysical Research Letters, 2020, 47, e2020GL089917.	4.0	12
28	Ongoing formation of felsic lower crustal channel by relamination in Zagros collision zone revealed from regional tomography. Scientific Reports, 2020, 10, 8224.	3.3	9
29	Analog and Numerical Experiments of Double Subduction Systems With Opposite Polarity in Adjacent Segments. Geochemistry, Geophysics, Geosystems, 2020, 21, e2020GC009035.	2.5	7
30	The role of pre-existing weak zones in the formation of the Himalaya and Tibetan plateau: 3-D thermomechanical modelling. Geophysical Journal International, 2020, 221, 1971-1983.	2.4	18
31	Lateral propagation–induced subduction initiation at passive continental margins controlled by preexisting lithospheric weakness. Science Advances, 2020, 6, eaaz1048.	10.3	54
32	Can Grain Size Reduction Initiate Transform Faults?—Insights From a 3â€Ð Numerical Study. Tectonics, 2020, 39, e2019TC005793.	2.8	15
33	Subduction Initiation by Plumeâ€Plateau Interaction: Insights From Numerical Models. Geochemistry, Geophysics, Geosystems, 2020, 21, e2020GC009119.	2.5	9
34	Plumeâ€Induced Subduction Initiation: Singleâ€5lab or Multiâ€5lab Subduction?. Geochemistry, Geophysics, Geosystems, 2020, 21, e2019GC008663.	2.5	28
35	Peel-back controlled lithospheric convergence explains the secular transitions in Archean metamorphism and magmatism. Earth and Planetary Science Letters, 2020, 538, 116224.	4.4	49
36	Oceanic crust recycling controlled by weakening at slab edges. Nature Communications, 2020, 11, 2009.	12.8	17

#	Article	IF	CITATIONS
37	Transient stripping of subducting slabs controls periodic forearc uplift. Nature Communications, 2020, 11, 1823.	12.8	49
38	Characteristics of earthquake ruptures and dynamic off-fault deformation on propagating faults. Solid Earth, 2020, 11, 1333-1360.	2.8	12
39	Seismic and Aseismic Fault Growth Lead to Different Fault Orientations. Journal of Geophysical Research: Solid Earth, 2019, 124, 8867-8889.	3.4	26
40	Stress-driven fluid flow controls long-term megathrust strength and deep accretionary dynamics. Scientific Reports, 2019, 9, 9714.	3.3	26
41	A Secondary Zone of Uplift Due to Megathrust Earthquakes. Pure and Applied Geophysics, 2019, 176, 4043-4068.	1.9	13
42	Geodynamics of the early Earth: Quest for the missing paradigm. Geology, 2019, 47, 1006-1007.	4.4	27
43	Isotopic and Petrologic Investigation, and a Thermomechanical Model of Genesis of Large-Volume Rhyolites in Arc Environments: Karymshina Volcanic Complex, Kamchatka, Russia. Frontiers in Earth Science, 2019, 6, .	1.8	10
44	The continuity equation. , 2019, , 12-25.		0
45	Density and gravity. , 2019, , 26-37.		0
46	Numerical solutions of partial differential equations. , 2019, , 38-49.		0
47	Stress and strain. , 2019, , 50-59.		0
48	The momentum equation. , 2019, , 60-72.		0
49	Viscous rheology of rocks. , 2019, , 73-81.		1
50	Numerical solutions of the momentum and continuity equations. , 2019, , 82-104.		2
51	The advection equation and marker-in-cell method. , 2019, , 105-127.		0
52	The heat conservation equation. , 2019, , 128-138.		0
53	Numerical solution of the heat conservation equation. , 2019, , 139-155.		1
54	2D thermomechanical code structure. , 2019, , 156-170.		1

#	Article	IF	CITATIONS
55	Elasticity and plasticity. , 2019, , 171-187.		0
56	2D implementation of visco-elasto-plasticity. , 2019, , 188-208.		0
57	2D thermomechanical modelling of inertial processes. , 2019, , 209-223.		0
58	Seismo-thermomechanical modelling. , 2019, , 224-239.		0
59	Hydro-thermomechanical modelling. , 2019, , 240-276.		0
60	Adaptive mesh refinement. , 2019, , 277-291.		0
61	The multigrid method. , 2019, , 292-318.		0
62	Programming of 3D problems. , 2019, , 319-339.		0
63	Numerical benchmarks. , 2019, , 340-368.		0
64	Design of 2D numerical geodynamic models. , 2019, , 369-405.		1
65	Variability of subducting slab morphologies in the mantle transition zone: Insight from petrological-thermomechanical modeling. Earth-Science Reviews, 2019, 196, 102874.	9.1	49
66	Growing primordial continental crust self-consistently in global mantle convection models. Gondwana Research, 2019, 73, 96-122.	6.0	31
67	Crustal melting beneath orogenic plateaus: Insights from 3-D thermo-mechanical modeling. Tectonophysics, 2019, 761, 1-15.	2.2	27
68	Near-ridge initiation of intraoceanic subduction: Effects of inheritance in 3D numerical models of the Wilson Cycle. Tectonophysics, 2019, 763, 1-13.	2.2	28
69	Plumeâ€Induced Breakup of a Subducting Plate: Microcontinent Formation Without Cessation of the Subduction Process. Geophysical Research Letters, 2019, 46, 3663-3675.	4.0	19
70	The Neoarchaean Limpopo Orogeny: Exhumation and Regional-Scale Gravitational Crustal Overturn Driven by a Granulite Diapir. Regional Geology Reviews, 2019, , 185-224.	1.2	11
71	A water budget dichotomy of rocky protoplanets from 26Al-heating. Nature Astronomy, 2019, 3, 307-313.	10.1	91
72	Late Orogenic Heating of (Ultra)High Pressure Rocks: Slab Rollback vs. Slab Breakoff. Geosciences (Switzerland), 2019, 9, 499.	2.2	33

#	Article	IF	CITATIONS
73	Understanding the isotopic and chemical evolution of Yellowstone hot spot magmatism using magmatic-thermomechanical modeling. Journal of Volcanology and Geothermal Research, 2019, 370, 13-30.	2.1	12
74	Magma ascent in planetesimals: Control by grain size. Earth and Planetary Science Letters, 2019, 507, 154-165.	4.4	31
75	On the formation of oceanic detachment faults and their influence on intra-oceanic subduction initiation: 3D thermomechanical modeling. Earth and Planetary Science Letters, 2019, 506, 195-208.	4.4	31
76	Bimodal seismicity in the Himalaya controlled by fault friction and geometry. Nature Communications, 2019, 10, 48.	12.8	78
77	3D numerical modelling of the Wilson cycle: structural inheritance of alternating subduction polarity. Geological Society Special Publication, 2019, 470, 439-461.	1.3	7
78	Thermomechanical Modeling of the Formation of a Multilevel, Crustalâ€ 5 cale Magmatic System by the Yellowstone Plume. Geophysical Research Letters, 2018, 45, 3873-3879.	4.0	54
79	Divergent plate motion drives rapid exhumation of (ultra)high pressure rocks. Earth and Planetary Science Letters, 2018, 491, 67-80.	4.4	35
80	Efficient cooling of rocky planets by intrusive magmatism. Nature Geoscience, 2018, 11, 322-327.	12.9	78
81	3D modeling of crustal shortening influenced by along-strike lithological changes: Implications for continental collision in the Western and Central Alps. Tectonophysics, 2018, 746, 425-438.	2.2	14
82	The Mechanism and Dynamics of Nâ€S Rifting in Southern Tibet: Insight From 3â€D Thermomechanical Modeling. Journal of Geophysical Research: Solid Earth, 2018, 123, 859-877.	3.4	20
83	Impact splash chondrule formation during planetesimal recycling. Icarus, 2018, 302, 27-43.	2.5	79
84	Variability of orogenic magmatism during Mediterranean-style continental collisions: A numerical modelling approach. Gondwana Research, 2018, 56, 119-134.	6.0	27
85	Dynamics of exhumation and deformation of HP-UHP orogens in double subduction-collision systems: Numerical modeling and implications for the Western Dabie Orogen. Earth-Science Reviews, 2018, 182, 68-84.	9.1	34
86	Precambrian ultra-hot orogenic factory: Making and reworking of continental crust. Tectonophysics, 2018, 746, 572-586.	2.2	49
87	Plume-induced continental rifting and break-up in ultra-slow extension context: Insights from 3D numerical modeling. Tectonophysics, 2018, 746, 121-137.	2.2	42
88	Stagnant lid tectonics: Perspectives from silicate planets, dwarf planets, large moons, and large asteroids. Geoscience Frontiers, 2018, 9, 103-119.	8.4	72
89	Dynamics of terrane accretion during seaward continental drifting and oceanic subduction: Numerical modeling and implications for the Jurassic crustal growth of the Lhasa Terrane, Tibet. Tectonophysics, 2018, 746, 212-228.	2.2	20
90	What drives metamorphism in early Archean greenstone belts? Insights from numerical modeling. Tectonophysics, 2018, 746, 587-601.	2.2	25

#	Article	IF	CITATIONS
91	Coupling SPH and thermochemical models of planets: Methodology and example of a Mars-sized body. Icarus, 2018, 301, 235-246.	2.5	65
92	Nucleation and evolution of ridge-ridge-ridge triple junctions: Thermomechanical model and geometrical theory. Tectonophysics, 2018, 746, 83-105.	2.2	37
93	Subduction initiation in nature and models: A review. Tectonophysics, 2018, 746, 173-198.	2.2	335
94	Relamination Styles in Collisional Orogens. Tectonics, 2018, 37, 224-250.	2.8	32
95	Plume-lithosphere interactions in rifted margin tectonic settings: Inferences from thermo-mechanical modelling. Tectonophysics, 2018, 746, 138-154.	2.2	20
96	Nonâ€uniform splitting of a single mantle plume by double cratonic roots: Insight into the origin of the central and southern East African Rift System. Terra Nova, 2018, 30, 125-134.	2.1	22
97	Seismic behaviour of mountain belts controlled by plate convergence rate. Earth and Planetary Science Letters, 2018, 482, 81-92.	4.4	78
98	Oblique continental rifting and long transform fault formation based on 3D thermomechanical numerical modeling. Tectonophysics, 2018, 746, 106-120.	2.2	18
99	The role of lateral strength contrasts in orogenesis: A 2D numerical study. Tectonophysics, 2018, 746, 549-561.	2.2	19
100	Subduction initiation dynamics along a transform fault control trench curvature and ophiolite ages. Geology, 2018, 46, 607-610.	4.4	69
101	Initiation of a Protoâ€ŧransform Fault Prior to Seafloor Spreading. Geochemistry, Geophysics, Geosystems, 2018, 19, 4744-4756.	2.5	18
102	Afar triple junction triggered by plume-assisted bi-directional continental break-up. Scientific Reports, 2018, 8, 14742.	3.3	30
103	Multi-terrane structure controls the contrasting lithospheric evolution beneath the western and central–eastern Tibetan plateau. Nature Communications, 2018, 9, 3780.	12.8	49
104	Alongâ€Axis Variations of Rift Width in a Coupled Lithosphereâ€Mantle System, Application to East Africa. Geophysical Research Letters, 2018, 45, 5362-5370.	4.0	20
105	An Invariant Rate―and Stateâ€Dependent Friction Formulation for Viscoeastoplastic Earthquake Cycle Simulations. Journal of Geophysical Research: Solid Earth, 2018, 123, 5018-5051.	3.4	64
106	Emplacement of metamorphic core complexes and associated geothermal systems controlled by slab dynamics. Earth and Planetary Science Letters, 2018, 498, 322-333.	4.4	36
107	Extensional Polarity Change in Continental Rifts: Inferences From 3â€D Numerical Modeling and Observations. Journal of Geophysical Research: Solid Earth, 2018, 123, 8073-8094.	3.4	23
108	Toward 4D modeling of orogenic belts: Example from the transpressive Zagros Fold Belt. Tectonophysics, 2017, 702, 82-89.	2.2	15

#	Article	IF	CITATIONS
109	Continental crust formation on early Earth controlled by intrusive magmatism. Nature, 2017, 545, 332-335.	27.8	174
110	Partitioning of crustal shortening during continental collision: 2â€Ð thermomechanical modeling. Journal of Geophysical Research: Solid Earth, 2017, 122, 592-606.	3.4	24
111	3D geodynamic models for the development of opposing continental subduction zones: The Hindu Kush–Pamir example. Earth and Planetary Science Letters, 2017, 480, 133-146.	4.4	31
112	Emergence of silicic continents as the lower crust peels off on a hot plate-tectonic Earth. Nature Geoscience, 2017, 10, 698-703.	12.9	90
113	Horizontal mantle flow controls subduction dynamics. Scientific Reports, 2017, 7, 7550.	3.3	41
114	Long-distance impact of Iceland plume on Norway's rifted margin. Scientific Reports, 2017, 7, 10408.	3.3	29
115	Crustal rheology controls on the Tibetan plateau formation during India-Asia convergence. Nature Communications, 2017, 8, 15992.	12.8	57
116	Stratigraphic signatures of forearc basin formation mechanisms. Geochemistry, Geophysics, Geosystems, 2017, 18, 2388-2410.	2.5	13
117	Modeling Craton Destruction by Hydrationâ€Induced Weakening of the Upper Mantle. Journal of Geophysical Research: Solid Earth, 2017, 122, 7449-7466.	3.4	30
118	Lithosphere delamination in continental collisional orogens: A systematic numerical study. Journal of Geophysical Research: Solid Earth, 2016, 121, 5186-5211.	3.4	116
119	The effects of short-lived radionuclides and porosity on the early thermo-mechanical evolution of planetesimals. Icarus, 2016, 274, 350-365.	2.5	89
120	Benchmarking numerical models of brittle thrust wedges. Journal of Structural Geology, 2016, 92, 140-177.	2.3	81
121	3D numerical modeling of mantle flow, crustal dynamics and magma genesis associated with slab roll-back and tearing: The eastern Mediterranean case. Earth and Planetary Science Letters, 2016, 442, 93-107.	4.4	101
122	Thermo-mechanical controls of flat subduction: Insights from numerical modeling. Gondwana Research, 2016, 40, 170-183.	6.0	48
123	3-D thermo-mechanical modeling of plume-induced subduction initiation. Earth and Planetary Science Letters, 2016, 453, 193-203.	4.4	39
124	Fluidâ€assisted deformation of the subduction interface: Coupled and decoupled regimes from 2â€Đ hydromechanical modeling. Journal of Geophysical Research: Solid Earth, 2016, 121, 6132-6149.	3.4	12
125	Crustal deformation dynamics and stress evolution during seamount subduction: Highâ€resolution 3â€Đ numerical modeling. Journal of Geophysical Research: Solid Earth, 2016, 121, 6880-6902.	3.4	68
126	Impact of sedimentation on evolution of accretionary wedges: Insights from high-resolution thermomechanical modeling. Tectonics, 2016, 35, 2828-2846.	2.8	15

#	Article	IF	CITATIONS
127	The role of lateral lithospheric strength heterogeneities in orogenic plateau growth: Insights from 3â€D thermoâ€mechanical modeling. Journal of Geophysical Research: Solid Earth, 2016, 121, 3118-3138.	3.4	32
128	Regimes of subduction and lithospheric dynamics in the Precambrian: 3D thermomechanical modelling. Gondwana Research, 2016, 37, 53-70.	6.0	88
129	Contrasted continental rifting via plume-craton interaction: Applications to Central East African Rift. Geoscience Frontiers, 2016, 7, 221-236.	8.4	68
130	Interplate deformation at earlyâ€stage oblique subduction: 3â€D thermomechanical numerical modeling. Tectonics, 2016, 35, 1610-1625.	2.8	9
131	Thermo-mechanical modeling of the obduction process based on the Oman Ophiolite case. Gondwana Research, 2016, 32, 1-10.	6.0	61
132	On the influence of the asthenospheric flow on the tectonics and topography at a collision-subduction transition zones: Comparison with the eastern Tibetan margin. Journal of Geodynamics, 2016, 100, 184-197.	1.6	36
133	Early Earth plume-lid tectonics: A high-resolution 3D numerical modelling approach. Journal of Geodynamics, 2016, 100, 198-214.	1.6	128
134	Numerical modeling of deep oceanic slab dehydration: Implications for the possible origin of far field intra-continental volcanoes in northeastern China. Journal of Asian Earth Sciences, 2016, 117, 328-336.	2.3	19
135	Decarbonation of subducting slabs: Insight from petrological–thermomechanical modeling. Gondwana Research, 2016, 36, 314-332.	6.0	30
136	2D thermomechanical modelling of continent–arc–continent collision. Gondwana Research, 2016, 32, 138-150.	6.0	28
137	Tectonic slicing of subducting oceanic crust along plate interfaces: Numerical modeling. Geochemistry, Geophysics, Geosystems, 2015, 16, 3505-3531.	2.5	46
138	How partial melting affects smallâ€scale convection in a plumeâ€fed sublithospheric layer beneath fastâ€moving plates. Geochemistry, Geophysics, Geosystems, 2015, 16, 3924-3945.	2.5	6
139	Tectonic overpressure and underpressure in lithospheric tectonics and metamorphism. Journal of Metamorphic Geology, 2015, 33, 785-800.	3.4	71
140	Material transportation and fluid-melt activity in the subduction channel: Numerical modeling. Science China Earth Sciences, 2015, 58, 1251-1268.	5.2	29
141	Supercomputer simulation of continental collisions in Precambrian: The effect of lithosphere thickness. Moscow University Geology Bulletin, 2015, 70, 77-83.	0.3	2
142	H 2 O-fluid-saturated melting of subducted continental crust facilitates exhumation of ultrahigh-pressure rocks in continental subduction zones. Earth and Planetary Science Letters, 2015, 428, 151-161.	4.4	40
143	Earthquake supercycle in subduction zones controlled by the width of the seismogenic zone. Nature Geoscience, 2015, 8, 471-474.	12.9	101
144	Dual continental rift systems generated by plume–lithosphere interaction. Nature Geoscience, 2015, 8, 388-392.	12.9	176

#	Article	IF	CITATIONS
145	Generation of felsic crust in the Archean: A geodynamic modeling perspective. Precambrian Research, 2015, 271, 198-224.	2.7	246
146	Geomorphological–thermo-mechanical modeling: Application to orogenic wedge dynamics. Tectonophysics, 2015, 659, 12-30.	2.2	52
147	Plate tectonics on the Earth triggered by plume-induced subduction initiation. Nature, 2015, 527, 221-225.	27.8	310
148	From continental rifting to seafloor spreading: Insight from 3D thermo-mechanical modeling. Gondwana Research, 2015, 28, 1329-1343.	6.0	44
149	Practical analytical solutions for benchmarking of 2-D and 3-D geodynamic Stokes problems with variable viscosity. Solid Earth, 2014, 5, 461-476.	2.8	37
150	Threeâ€dimensional simulations of the southern polar giant impact hypothesis for the origin of the Martian dichotomy. Geophysical Research Letters, 2014, 41, 8736-8743.	4.0	71
151	Implementation of a multigrid solver on a GPU for Stokes equations with strongly variable viscosity based on Matlab and CUDA. International Journal of High Performance Computing Applications, 2014, 28, 50-60.	3.7	30
152	Lead transport in intra-oceanic subduction zones: 2D geochemical–thermo-mechanical modeling of isotopic signatures. Lithos, 2014, 208-209, 265-280.	1.4	32
153	Numerical models of the thermomechanical evolution of planetesimals: Application to the acapulcoiteâ€odranite parent body. Meteoritics and Planetary Science, 2014, 49, 1083-1099.	1.6	59
154	Contrasting styles of Phanerozoic and Precambrian continental collision. Gondwana Research, 2014, 25, 522-545.	6.0	244
155	Precambrian geodynamics: Concepts and models. Gondwana Research, 2014, 25, 442-463.	6.0	262
156	Plume-induced crustal convection: 3D thermomechanical model and implications for the origin of novae and coronae on Venus. Earth and Planetary Science Letters, 2014, 391, 183-192.	4.4	78
157	From oceanic plateaus to allochthonous terranes: Numerical modelling. Gondwana Research, 2014, 25, 494-508.	6.0	82
158	Modeling the seismic cycle in subduction zones: The role and spatiotemporal occurrence of offâ€megathrust earthquakes. Geophysical Research Letters, 2014, 41, 1194-1201.	4.0	51
159	Slab detachment in laterally varying subduction zones: 3-D numerical modeling. Geophysical Research Letters, 2014, 41, 1951-1956.	4.0	82
160	Subduction of fracture zones controls mantle melting and geochemical signature above slabs. Nature Communications, 2014, 5, 5095.	12.8	51
161	Subduction initiates at straight passive margins. Geology, 2014, 42, 331-334.	4.4	32
162	Asymmetric three-dimensional topography over mantle plumes. Nature, 2014, 513, 85-89.	27.8	190

#	Article	IF	CITATIONS
163	Driving the upper plate surface deformation by slab rollback and mantle flow. Earth and Planetary Science Letters, 2014, 405, 110-118.	4.4	120
164	Boris Kaus receives 2012 Paul Niggli Medal. Swiss Journal of Geosciences, 2014, 107, 129-131.	1.2	0
165	Deep plate serpentinization triggers skinning of subducting slabs. Geology, 2014, 42, 723-726.	4.4	20
166	Dependence of mid-ocean ridge morphology on spreading rate in numerical 3-D models. Gondwana Research, 2014, 25, 270-283.	6.0	31
167	Numerical approach to the Stokes problem with high contrasts in viscosity. Applied Mathematics and Computation, 2014, 235, 17-25.	2.2	5
168	Influence of lithospheric mantle stratification on craton extension: Insight from two-dimensional thermo-mechanical modeling. Tectonophysics, 2014, 631, 50-64.	2.2	57
169	3D effects of strain vs. velocity weakening on deformation patterns in accretionary wedges. Tectonophysics, 2014, 615-616, 122-141.	2.2	29
170	Geodynamic regimes of intra-oceanic subduction: Implications for arc extension vs. shortening processes. Gondwana Research, 2014, 25, 546-560.	6.0	43
171	Formation and Exhumation of Ultrahigh-Pressure Terranes. Elements, 2013, 9, 289-293.	0.5	55
172	Intracratonic geodynamics. Gondwana Research, 2013, 24, 838-848.	6.0	44
173	Collision of continental corner from 3-D numerical modeling. Earth and Planetary Science Letters, 2013, 380, 98-111.	4.4	134
174	Fourâ€dimensional numerical modeling of crustal growth at active continental margins. Journal of Geophysical Research: Solid Earth, 2013, 118, 4682-4698.	3.4	18
175	The seismic cycle at subduction thrusts: Insights from seismoâ€thermoâ€mechanical models. Journal of Geophysical Research: Solid Earth, 2013, 118, 6183-6202.	3.4	100
176	Oblique subduction modelling indicates along-trench tectonic transport of sediments. Nature Communications, 2013, 4, 2456.	12.8	35
177	Testing the influence of far-field topographic forcing on subduction initiation at a passive margin. Tectonophysics, 2013, 608, 517-524.	2.2	41
178	Initiation of transform faults at rifted continental margins: 3D petrological-thermomechanical modeling and comparison to the Woodlark Basin. Petrology, 2013, 21, 550-560.	0.9	37
179	Numerical modeling of eastern Tibetan-type margin: Influences of surface processes, lithospheric structure and crustal rheology. Gondwana Research, 2013, 24, 1091-1107.	6.0	17
180	Generation of new continental crust by sublithospheric silicic-magma relamination in arcs: A test of Taylor's andesite model. Gondwana Research, 2013, 23, 1554-1566.	6.0	130

#	Article	IF	CITATIONS
181	Mafic injection as a trigger for felsic magmatism: A numerical study. Geochemistry, Geophysics, Geosystems, 2013, 14, 1910-1928.	2.5	49
182	Numerical modeling of geochemical variations caused by crustal relamination. Geochemistry, Geophysics, Geosystems, 2013, 14, 470-487.	2.5	58
183	Highâ€resolution 3D numerical modeling of thrust wedges: Influence of décollement strength on transfer zones. Geochemistry, Geophysics, Geosystems, 2013, 14, 1131-1155.	2.5	50
184	Paradigms, new and old, for ultrahigh-pressure tectonism. Tectonophysics, 2013, 603, 79-88.	2.2	122
185	Three-dimensional thermomechanical modeling of oceanic spreading initiation and evolution. Physics of the Earth and Planetary Interiors, 2013, 214, 35-52.	1.9	119
186	Slab detachment during continental collision: Influence of crustal rheology and interaction with lithospheric delamination. Tectonophysics, 2013, 602, 124-140.	2.2	96
187	Small-scale convection in a plume-fed low-viscosity layer beneath a moving plate. Geophysical Journal International, 2013, 194, 591-610.	2.4	22
188	Layered structure of the lithospheric mantle changes dynamics of craton extension. Geophysical Research Letters, 2013, 40, 5861-5866.	4.0	24
189	The seismic cycle at subduction thrusts: 2. Dynamic implications of geodynamic simulations validated with laboratory models. Journal of Geophysical Research: Solid Earth, 2013, 118, 1502-1525.	3.4	81
190	Dynamics of outerâ€rise faulting in oceanic ontinental subduction systems. Geochemistry, Geophysics, Geosystems, 2013, 14, 2310-2327.	2.5	65
191	Porous fluid flow enables oceanic subduction initiation on Earth. Geophysical Research Letters, 2013, 40, 5671-5676.	4.0	92
192	Formation mechanism of steep convergent intracontinental margins: Insights from numerical modeling. Geophysical Research Letters, 2013, 40, 2000-2005.	4.0	18
193	An adaptive staggered grid finite difference method for modeling geodynamic Stokes flows with strongly variable viscosity. Geochemistry, Geophysics, Geosystems, 2013, 14, 1200-1225.	2.5	43
194	GPU Implementation of Multigrid Solver for Stokes Equation with Strongly Variable Viscosity. Lecture Notes in Earth System Sciences, 2013, , 321-333.	0.6	6
195	Exhumation mechanisms of meltâ€bearing ultrahigh pressure crustal rocks during collision of spontaneously moving plates. Journal of Metamorphic Geology, 2012, 30, 927-955.	3.4	122
196	Crustal growth at active continental margins: Numerical modeling. Physics of the Earth and Planetary Interiors, 2012, 192-193, 1-20.	1.9	131
197	Fluid flow during slab unbending and dehydration: Implications for intermediateâ€depth seismicity, slab weakening and deep water recycling. Geochemistry, Geophysics, Geosystems, 2012, 13, .	2.5	146
198	Dynamics of slab detachment. Geochemistry, Geophysics, Geosystems, 2012, 13, .	2.5	86

#	Article	IF	CITATIONS
199	A free plate surface and weak oceanic crust produce singleâ€sided subduction on Earth. Geophysical Research Letters, 2012, 39, .	4.0	147
200	Thermomechanical modeling of slab eduction. Journal of Geophysical Research, 2012, 117, .	3.3	58
201	Delamination in collisional orogens: Thermomechanical modeling. Journal of Geophysical Research, 2012, 117, .	3.3	111
202	Bimodal behavior of extended continental lithosphere: Modeling insight and application to thermal history of migmatitic core complexes. Tectonophysics, 2012, 579, 88-103.	2.2	35
203	A comparison of numerical surface topography calculations in geodynamic modelling: an evaluation of the †sticky air' method. Geophysical Journal International, 2012, 189, 38-54.	2.4	301
204	Intraoceanic subduction of "heterogeneous―oceanic lithosphere in narrow basins: 2D numerical modeling. Lithos, 2012, 140-141, 234-251.	1.4	24
205	Origin and models of oceanic transform faults. Tectonophysics, 2012, 522-523, 34-54.	2.2	80
206	Initiation of Rayleigh–Taylor instabilities in intra-cratonic settings. Tectonophysics, 2012, 514-517, 146-155.	2.2	48
207	Tectonic blocks in serpentinite mélange (eastern Cuba) reveal large-scale convective flow of the subduction channel. Geology, 2011, 39, 79-82.	4.4	77
208	Discretization errors and free surface stabilization in the finite difference and marker-in-cell method for applied geodynamics: A numerical study. Geochemistry, Geophysics, Geosystems, 2011, 12, n/a-n/a.	2.5	102
209	Subduction of young oceanic plates: A numerical study with application to aborted thermal-chemical plumes. Geochemistry, Geophysics, Geosystems, 2011, 12, n/a-n/a.	2.5	18
210	Flat versus steep subduction: Contrasting modes for the formation and exhumation of high- to ultrahigh-pressure rocks in continental collision zones. Earth and Planetary Science Letters, 2011, 301, 65-77.	4.4	96
211	Arc–Continent Collision: The Making of an Orogen. Frontiers in Earth Sciences, 2011, , 477-493.	0.1	42
212	Intra-oceanic Subduction Zones. Frontiers in Earth Sciences, 2011, , 23-51.	0.1	38
213	Future directions in subduction modeling. Journal of Geodynamics, 2011, 52, 344-378.	1.6	227
214	Influences of the buoyancy of partially molten rock on 3-D plume patterns and melt productivity above retreating slabs. Physics of the Earth and Planetary Interiors, 2011, 185, 112-121.	1.9	21
215	Granite emplacement and the retrograde P-T-fluid evolution of Neoarchean granulites from the Central Zone of the Limpopo Complex. , 2011, , .		5
216	Formation and evolution of Precambrian granulite terranes: A gravitational redistribution model. , 2011, , .		5

#	Article	IF	CITATIONS
217	Geodynamic regimes of subduction under an active margin: effects of rheological weakening by fluids and melts. Journal of Metamorphic Geology, 2011, 29, 7-31.	3.4	270
218	Numerical modelling of spontaneous slab breakoff and subsequent topographic response. Tectonophysics, 2011, 502, 244-256.	2.2	291
219	Origin of the martian dichotomy and Tharsis from a giant impact causing massive magmatism. Icarus, 2011, 215, 346-357.	2.5	99
220	Melt evolution above a spontaneously retreating subducting slab in a three-dimensional model. Journal of Earth Science (Wuhan, China), 2011, 22, 137-142.	3.2	8
221	Protocore destabilization in planetary embryos formed by cold accretion: Feedbacks from non-Newtonian rheology and energy dissipation. Icarus, 2011, 213, 24-42.	2.5	4
222	Numerical analysis of subduction initiation risk along the Atlantic American passive margins. Geology, 2011, 39, 463-466.	4.4	47
223	Samovar: a thermomechanical code for modeling of geodynamic processes in the lithosphere—application to basin evolution. Arabian Journal of Geosciences, 2010, 3, 477-497.	1.3	2
224	Subduction styles in the Precambrian: Insight from numerical experiments. Lithos, 2010, 116, 209-229.	1.4	351
225	Influence of tectonic overpressure on <i>P–T</i> paths of HP–UHP rocks in continental collision zones: thermomechanical modelling. Journal of Metamorphic Geology, 2010, 28, 227-247.	3.4	118
226	Ternary system H2O-CO2-NaCl at high T-P parameters: An empirical mixing model. Geochemistry International, 2010, 48, 446-455.	0.7	64
227	Small-Scale Mantle Convection Produces Stratigraphic Sequences in Sedimentary Basins. Science, 2010, 329, 827-830.	12.6	74
228	Numerical modelling of spontaneous slab breakoff dynamics during continental collision. Geological Society Special Publication, 2010, 332, 99-114.	1.3	40
229	Melting Relations of MORB-Sediment Melanges in Underplated Mantle Wedge Plumes; Implications for the Origin of Cordilleran-type Batholiths. Journal of Petrology, 2010, 51, 1267-1295.	2.8	179
230	Subduction initiation at passive margins: Numerical modeling. Journal of Geophysical Research, 2010, 115, .	3.3	136
231	A simple three-dimensional model of thermo–chemical convection in the mantle wedge. Earth and Planetary Science Letters, 2010, 290, 311-318.	4.4	28
232	Dynamical Instability Produces Transform Faults at Mid-Ocean Ridges. Science, 2010, 329, 1047-1050.	12.6	130
233	Translithospheric Mantle Diapirism: Geological Evidence and Numerical Modelling of the Kondyor Zoned Ultramafic Complex (Russian Far-East). Journal of Petrology, 2009, 50, 289-321.	2.8	90
234	Ordovician ferrosilicic magmas: Experimental evidence for ultrahigh temperatures affecting a metagreywacke source. Gondwana Research, 2009, 16, 622-632.	6.0	27

#	Article	IF	CITATIONS
235	Diffusion of divalent cations in garnet: multi-couple experiments. Contributions To Mineralogy and Petrology, 2009, 157, 573-592.	3.1	48
236	Deep slab hydration induced by bending-related variations in tectonic pressure. Nature Geoscience, 2009, 2, 790-793.	12.9	289
237	Numerical modeling of protocore destabilization during planetary accretion: Methodology and results. Icarus, 2009, 204, 732-748.	2.5	50
238	Numerical modeling of intraoceanic arc growth. Moscow University Geology Bulletin, 2009, 64, 230-243.	0.3	1
239	Coupled and decoupled regimes of continental collision: Numerical modeling. Earth and Planetary Science Letters, 2009, 278, 337-349.	4.4	98
240	Rheological controls on the terrestrial core formation mechanism. Geochemistry, Geophysics, Geosystems, 2009, 10, .	2.5	18
241	Threeâ€dimensional dynamics of hydrous thermal hemical plumes in oceanic subduction zones. Geochemistry, Geophysics, Geosystems, 2009, 10, .	2.5	112
242	Polyphase formation and exhumation of high―to ultrahighâ€pressure rocks in continental subduction zone: Numerical modeling and application to the Sulu ultrahighâ€pressure terrane in eastern China. Journal of Geophysical Research, 2009, 114, .	3.3	66
243	Dynamic effects of aseismic ridge subduction: numerical modelling. European Journal of Mineralogy, 2009, 21, 649-661.	1.3	100
244	Fault-induced seismic anisotropy by hydration in subducting oceanic plates. Nature, 2008, 455, 1097-1100.	27.8	271
245	Styles of post-subduction collisional orogeny: Influence of convergence velocity, crustal rheology and radiogenic heat production. Lithos, 2008, 103, 257-287.	1.4	222
246	Magmatic implications of mantle wedge plumes: Experimental study. Lithos, 2008, 103, 138-148.	1.4	138
247	Transient hot channels: Perpetrating and regurgitating ultrahigh-pressure, high-temperature crust–mantle associations in collision belts. Lithos, 2008, 103, 236-256.	1.4	218
248	Why is terrestrial subduction one-sided?. Geology, 2008, 36, 43.	4.4	221
249	Dynamics of double subduction: Numerical modeling. Physics of the Earth and Planetary Interiors, 2008, 171, 280-295.	1.9	90
250	Numerical modelling of crustal growth in intraoceanic volcanic arcs. Physics of the Earth and Planetary Interiors, 2008, 171, 336-356.	1.9	146
251	A benchmark comparison of spontaneous subduction models—Towards a free surface. Physics of the Earth and Planetary Interiors, 2008, 171, 198-223.	1.9	361
252	Subduction initiation by thermal–chemical plumes: Numerical studies. Physics of the Earth and Planetary Interiors, 2008, 171, 296-312.	1.9	155

#	Article	IF	CITATIONS
253	Recent advances in computational geodynamics: Theory, numerics and applications. Physics of the Earth and Planetary Interiors, 2008, 171, 2-6.	1.9	3
254	Sapphirine-bearing assemblages in the system MgOAl2O3SiO2: a continuing ambiguity. European Journal of Mineralogy, 2008, 20, 721-734.	1.3	15
255	Intrusion of ultramafic magmatic bodies into the continental crust: Numerical simulation. Physics of the Earth and Planetary Interiors, 2007, 160, 124-142.	1.9	131
256	Robust characteristics method for modelling multiphase visco-elasto-plastic thermo-mechanical problems. Physics of the Earth and Planetary Interiors, 2007, 163, 83-105.	1.9	369
257	Physical controls of magmatic productivity at Pacific-type convergent margins: Numerical modelling. Physics of the Earth and Planetary Interiors, 2007, 163, 209-232.	1.9	117
258	Densities of metapelitic rocks at high to ultrahigh pressure conditions: What are the geodynamic consequences?. Earth and Planetary Science Letters, 2007, 256, 12-27.	4.4	70
259	Non-Newtonian rheology of crystal-bearing magmas and implications for magma ascent dynamics. Earth and Planetary Science Letters, 2007, 264, 402-419.	4.4	390
260	Growth and mixing dynamics of mantle wedge plumes. Geology, 2007, 35, 587.	4.4	91
261	Asthenospheric upwelling, oceanic slab retreat, and exhumation of UHP mantle rocks: Insights from Greater Antilles. Geophysical Research Letters, 2007, 34, .	4.0	87
262	Metamorphic rocks of the Samerberg complex, Eastern Alps: 2. P-T paths and the problem of a geodynamic model. Petrology, 2007, 15, 369-385.	0.9	1
263	Order/disorder phase transition in cordierite and its possible relationship to the development of symplectite reaction textures in granulites. Petrology, 2007, 15, 427-440.	0.9	6
264	Influence of lower crustal rheology on styles of continental collision: numerical modeling and observations. , 2007, , .		0
265	Large-scale rigid-body rotation in the mantle wedge and its implications for seismic tomography. Geochemistry, Geophysics, Geosystems, 2006, 7, n/a-n/a.	2.5	45
266	The numerical sandbox: comparison of model results for a shortening and an extension experiment. Geological Society Special Publication, 2006, 253, 29-64.	1.3	84
267	Seismic implications of mantle wedge plumes. Physics of the Earth and Planetary Interiors, 2006, 156, 59-74.	1.9	190
268	P-T paths and problems of high-temperature polymetamorphism. Petrology, 2006, 14, 117-153.	0.9	21
269	Two-dimensional numerical modeling of tectonic and metamorphic histories at active continental margins. International Journal of Earth Sciences, 2006, 95, 250-274.	1.8	245
270	The role of viscous heating in Barrovian metamorphism of collisional orogens: thermomechanical models and application to the Lepontine Dome in the Central Alps. Journal of Metamorphic Geology, 2005, 23, 75-95.	3.4	355

#	Article	IF	CITATIONS
271	P-T-fluid evolution in the Mahalapye Complex, Limpopo high-grade terrane, eastern Botswana. Journal of Metamorphic Geology, 2005, 23, 313-334.	3.4	31
272	Pre-collisional high pressure metamorphism and nappe tectonics at active continental margins: a numerical simulation. Terra Nova, 2005, 17, 102-110.	2.1	179
273	Thermodynamic modeling of solubility and speciation of silica in H2O-SiO2 fluid up to 1300C and 20 kbar based on the chain reaction formalism. European Journal of Mineralogy, 2005, 17, 269-283.	1.3	46
274	Blueschists and Blue Amphiboles: How much Subduction do they Need?. International Geology Review, 2005, 47, 688-702.	2.1	16
275	Structural and P-T Evolution of a Major Cross Fold in the Central Zone of the Limpopo High-Grade Terrain, South Africa. Journal of Petrology, 2004, 45, 1413-1439.	2.8	49
276	Metapelites of the Kanskiy Granulite Complex (Eastern Siberia): Kinked P-T Paths and Geodynamic Model. Journal of Petrology, 2004, 45, 1393-1412.	2.8	50
277	Inherent gravitational instability of hot continental crust: Implications for doming and diapirism in granulite facies terrains. , 2004, , .		62
278	A counterclockwise PTt path of high-pressure/low-temperature rocks from the Coastal Cordillera accretionary complex of south-central Chile: constraints for the earliest stage of subduction mass flow. Lithos, 2004, 75, 283-310.	1.4	112
279	Visualization of multi-scale dynamics of hydrous cold plumes at subduction zones. Visual Geosciences, 2004, 9, 59-59.	0.5	45
280	Semi-empirical Gibbs free energy formulations for minerals and fluids for use in thermodynamic databases of petrological interest. Physics and Chemistry of Minerals, 2004, 31, 429.	0.8	59
281	The application of multidimensional wavelets to unveiling multi-phase diagrams and in situ physical properties of rocks. Earth and Planetary Science Letters, 2004, 223, 49-64.	4.4	53
282	Thermomechanical modelling of slab detachment. Earth and Planetary Science Letters, 2004, 226, 101-116.	4.4	257
283	Dynamical causes for incipient magma chambers above slabs. Geology, 2004, 32, 89.	4.4	127
284	"Cold―diapirs triggered by intrusion of the Bushveld Complex: Insight from two-dimensional numerical modeling. , 2004, , .		7
285	Characteristics-based marker-in-cell method with conservative finite-differences schemes for modeling geological flows with strongly variable transport properties. Physics of the Earth and Planetary Interiors, 2003, 140, 293-318.	1.9	430
286	Rayleigh–Taylor instabilities from hydration and melting propel â€~cold plumes' at subduction zones. Earth and Planetary Science Letters, 2003, 212, 47-62.	4.4	494
287	Mylonitization and decomposition of Garnet: Evidence for rapid deformation and entrainment of Mantle Garnet-Harzburgite by Kimberlite Magma, K1 Pipe, Venetia Mine, South Africa. South African Journal of Geology, 2003, 106, 231-242.	1.2	11
288	Cold fingers in a hot magma: Numerical modeling of country-rock diapirs in the Bushveld Complex, South Africa. Geology, 2003, 31, 753.	4.4	28

#	Article	IF	CITATIONS
289	Thermal regime and gravitational instability of multi-layered continental crust: implications for the buoyant exhumation of high-grade metamorphic rocks. European Journal of Mineralogy, 2002, 14, 687-699.	1.3	39
290	Exhumation rates of high pressure metamorphic rocks in subduction channels: The effect of Rheology. Geophysical Research Letters, 2002, 29, 102-1-102-4.	4.0	103
291	Exhumation of high-pressure metamorphic rocks in a subduction channel: A numerical simulation. Tectonics, 2002, 21, 6-1-6-19.	2.8	689
292	Numerical modelling of PT-paths related to rapid exhumation of high-pressure rocks from the crustal root in the Variscan Erzgebirge Dome (Saxony/Germany). Journal of Geodynamics, 2002, 33, 281-314.	1.6	79
293	Inherent gravitational instability of thickened continental crust with regionally developed low- to medium-pressure granulite facies metamorphism. Earth and Planetary Science Letters, 2001, 190, 221-235.	4.4	76
294	P -T conditions of decompression of the Limpopo high-grade terrane: record from shear zones. Journal of Metamorphic Geology, 2001, 19, 249-268.	3.4	44
295	Structural-metamorphic evolution of the Southern Yenisey Range of Eastern Siberia: implications for the emplacement of the Kanskiy granulite Complex. Mineralogy and Petrology, 2000, 69, 35-67.	1.1	24
296	Comparative petrology and metamorphic evolution of the Limpopo (South Africa) and Lapland (Fennoscandia) high-grade terrains. Mineralogy and Petrology, 2000, 69, 0069-0107.	1.1	52
297	P - T paths and tectonic evolution of shear zones separating high-grade terrains from cratons: examples from Kola Peninsula (Russia) and Limpopo Region (South Africa). Mineralogy and Petrology, 2000, 69, 109-142.	1.1	37
298	Mobility of components in metasomatic transformation and partial melting of gneisses: an example from Sri Lanka. Contributions To Mineralogy and Petrology, 2000, 140, 212-232.	3.1	60
299	Two-dimensional numerical modeling of pressure–temperature-time paths for the exhumation of some granulite facies terrains in the Precambrian. Journal of Geodynamics, 2000, 30, 17-35.	1.6	102
300	Fluid control of charnockitization. Chemical Geology, 1993, 108, 175-186.	3.3	45
301	THE FLUID REGIME OF METAMORPHISM AND THE CHARNOCKITE REACTION IN GRANULITES: A REVIEW. International Geology Review, 1992, 34, 1-58.	2.1	16
302	Petrology and retrograde P-T path in granulites of the Kanskaya formation, Yenisey range, Eastern Siberia. Journal of Metamorphic Geology, 1989, 7, 599-617.	3.4	51
303	Contrasting transform and passive margin subsidence history and heat flow evolution: insights from 3D thermo-mechanical modelling. Geological Society Special Publication, 0, , SP524-2021-94.	1.3	2
304	Bathymetric Highs Control the Along-Strike Variations of the Manila Trench: 2D Numerical Modeling. Frontiers in Earth Science, 0, 10, .	1.8	1